JGR Biogeosciences

RESEARCH ARTICLE
10.1029/2018JG004953

# Use of Surface Motion Characteristics Determined by InSAR to Assess Peatland Condition

**Lubna Alshammari[1,2], Doreen S. Boyd[3], Andrew Sowter[4], Chris Marshall[1], Roxane Andersen[5], Peter Gilbert[5], Stuart Marsh[1], and David J. Large[1]**

[1]Faculty of Engineering, University of Nottingham, Nottingham, UK, [2]Faculty of Engineering, Al-Mustansiriya University, Baghdad, Iraq, [3]School of Geography, University of Nottingham, Nottingham, UK, [4]Geomatic Ventures Limited, Nottingham Geospatial Building, Nottingham, UK, [5]Environmental Research Institute, North Highland College, University of the Highlands and Islands, Thurso, UK

**Abstract** Peatland surface motion is a key property of peatland that relates to condition. However, field-based techniques to measure surface motion are not cost-effective over large areas and long time periods. An alternative method that can quantify peatland surface motion over large areas is interferometric synthetic aperture radar. Although field validation of the accuracy of this method is difficult, the value of interferometric synthetic aperture radar (InSAR) as a means of quantifying peat condition can be tested. To achieve this, the characteristics of InSAR time series measured over an18-month period at 22 peatland sites in the Flow Country northern Scotland were compared to site condition assessment based on plant functional type and site management history. Sites in good condition dominated by *Sphagnum* display long-term stability or growth and a seasonal cycle with maximum uplift and subsidence in August–November and April–June, respectively. Drier and partially drained sites dominated by shrubs display long-term subsidence with maximum uplift and subsidence in July–October and February–June, respectively. Heavily degraded sites with large bare peat extent display subsidence with no distinct seasonal oscillations. Seasonal oscillation in surface motion at sites with a dominant nonvascular plant community is interpreted as resulting from changes in seasonal evaporative demand. On sites with extensive vascular plants cover and falling water table, surface oscillations are interpreted as representing sustained drawdown during the growing season and subsequent recharge in late winter. This study highlights the potential to use InSAR to characterize peatland condition and provide a new view of the surface dynamics of peatland landscapes.

**Plain Language Summary** Peatlands contain one third of all soil carbon despite covering only 3% of the Earth's land area. Peatlands in good condition cool climate through carbon sequestration and provide a range of other benefits such as water regulation and support of biodiversity. All these are compromised by peatland degradation, with severe costs to society. Given the global extent and remoteness of many peatlands, tools are needed to reliably assess peatland condition and inform future management. This research assesses the potential to use remote sensing of surface motion to measure peatland condition. The surface of peatland is known to move in response to change in water or gas in the peat but is notoriously difficult to measure. Our research provides the first indication that surface motion measured by satellite radar can differentiate peatland condition categories effectively. Wet, mossy peatland in good condition displays a strong and distinctive seasonal cycle falling mid summer and rising in midwinter. Drier shrubby peatland has a completely different pattern of motion, with the surface falling in late summer and rising to a peak in late spring. This evidence opens new possibilities of using satellite radar to provide a global view of peatland. With further development, this technique could enable rapid and continuous assessment of the condition of peatland and therefore inform management decisions.

**Key Points:**
- Interferometric satellite radar time series can be used to characterize peat surface motion
- Peatland sites conditions can consistently and reliably be inferred on the basis of these time series properties
- This technique brings about a new view of peatland dynamics, and our approach paves the way for peatland condition monitoring over whole regions and countries

**Supporting Information:**
- Supporting Information S1
- Data Set S1
- Figure S1

**Correspondence to:**
D. J. Large,
david.large@nottingham.ac.uk

**Citation:**
Alshammari, L., Boyd, D. S., Sowter, A., Marshall, C., Andersen, R., Gilbert, P., et al. (2020). Use of surface motion characteristics determined by InSAR to assess peatland condition. *Journal of Geophysical Research: Biogeosciences*, *125*, e2018JG004953. https://doi.org/10.1029/2018JG004953

Received 23 NOV 2018
Accepted 12 NOV 2019
Accepted article online 26 DEC 2019

**Author Contributions:**
**Conceptualization:** Doreen S. Boyd, Andrew Sowter, David J. Large
**Formal analysis:** Lubna Alshammari, Doreen S. Boyd, Roxane Andersen
**Funding acquisition:** Lubna Alshammari, Andrew Sowter, David J. Large
**Investigation:** Roxane Andersen, Peter Gilbert
**Methodology:** Lubna Alshammari, Doreen S. Boyd, Andrew Sowter, Chris
*(continued)*



## 1. Introduction

Peatland surfaces are particularly dynamic (Ingram, 1983) and move in response to changes in the mass of water, gas, and organic matter stored within the peat body. Changes in this mass are caused by both seasonal and long-term environmental change in evapotranspiration, rainfall, atmospheric pressure, drainage, temperature, decay, and loading (Fritz et al., 2008; Kennedy & Price, 2005). The observed mechanical response of the peat is, in turn, related to the nonlinear elastic properties of the peat matrix, its gas content, and state of decay (Kennedy & Price, 2005; Reeve et al., 2013). Thus, surface motion of peat results from four

Marshall, Roxane Andersen, Peter Gilbert

**Project administration:** Doreen S. Boyd, Andrew Sowter
**Software:** Andrew Sowter
**Supervision:** Doreen S. Boyd, Andrew Sowter, Stuart Marsh
**Validation:** Chris Marshall, Roxane Andersen
**Writing - original draft:** David J. Large
**Writing – review & editing:** Lubna Alshammari, Doreen S. Boyd, Andrew Sowter, Chris Marshall, Roxane Andersen, Stuart Marsh, David J. Large

contributing factors (Fritz et al., 2008; Kennedy & Price, 2005): growth because of accumulation; irreversible subsidence caused by drainage, compression, and decay of organic matter; and reversible elastic deformation of the peat matrix due to seasonal and shorter-term variation in the mass of water and gas stored within the peat. Each of these contributing factors relates to peat condition, and this in turn relates to ecosystem services provided by peatlands (Glenk et al., 2014). In short, long-term peat growth is indicative of carbon sequestration and good condition; long-term subsidence is indicative of carbon loss and poor condition; and reversible seasonal deformation is sensitive to the elastic properties of the peat matrix which are in turn sensitive to degradation (Kennedy & Price, 2005).

To some extent, the relationship between condition and surface motion is intuitive. Taking the peatlands of the Flow Country, Scotland (which has the largest extent of blanket bogs in Europe), as a worked example, a degraded, drained, dense peat is expected to display a markedly different surface motion dynamic in comparison to low-density water and gas saturated young *Sphagnum* peat. Yet detailed studies of peatland surface motion, beyond simple measures of subsidence, are rare (e.g., Fritz et al., 2008; Kennedy & Price, 2005; Reeve et al., 2013) and tend to be confined to a small spatial scale because of the logistical and financial challenges posed by large-scale field surveys. An ability to observe surface motion of peatlands continuously and reliably across large geographical regions, and in turn learn of their condition, would enhance understanding of peatland systems and their role in global environmental change and thus inform future management and conservation decisions pertaining to this fragile but valuable landscape (Lees et al., 2018).

Recent progress in Earth Observation, both in sensor technologies and algorithmic advances, means that peatland surface motion can now be measured using satellite interferometric synthetic aperture radar (InSAR) techniques (Fiaschi et al., 2019; Kim et al., 2017; Zhou et al., 2016). In particular, a recent development in satellite InSAR methods, the Intermittent Small Baseline Subset (ISBAS) differential InSAR (DInSAR) algorithm (Bateson et al., 2015; Gee et al., 2016; Sowter et al., 2013; Sowter et al., 2016) that has been successful in measuring surface motion of peat surfaces using data from the Sentinel 1 C-band radar sensor (Alshammari et al., 2018; Cigna et al., 2014), creates the potential to investigate in detail peat surface motion on an unprecedented scale. Unlike previous InSAR techniques, which provide patchy, unusable coverage in rural and forested areas, the ISBAS algorithm affords near continuous coverage across almost all rural land-cover classes—indeed ISBAS has been shown to be able to provide a level of coverage in rural areas in excess of most other InSAR methods (Gee et al., 2016), including SqueeSAR (Grebby et al., 2019). Trials have established that millimetric precision can be obtained on rates of 0.1 to >2 cm/year in peatland with a spatial resolution up to 100 × 100 m (Cigna et al., 2014) a range suited to quantifying the long-term rates of change observed in northern peatlands (Waddington & McNeill, 2002; Wosten et al., 1997).

It must be emphasized that the ISBAS method is a coherent scatterer technique where a pixel is likely to contain a large distributed group of small scatterers of similar size whose response is constant over time. For synthetic aperture radar (SAR) resolutions down to 10 m in size, this will be true for most natural scatterers such as forests and agricultural land (Even & Schultz, 2018) and probably even more so for a homogeneous peatland surface. Note that this is in marked contrast to a permanent scatterer (PS) approach (e.g., Ferretti et al., 2000; Ferretti et al., 2001) where it is assumed that there is a single dominant scatterer within a resolution cell. For this reason, a PS method is less likely to succeed over a natural surface. Forest canopies are often assumed to be inpenetrable to C-band radar, despite there being several studies to the contrary based upon the application of interferograms in densely canopies regions (Mohammadimanesh et al., 2018; Wdowinski & Hong, 2015). It is clear, though, that the InSAR coherence of forests is highly intermittent which is generally a barrier to most time series InSAR methods that require a consistent response. However, this lack of constancy is not a barrier to the ISBAS method, which has been designed specifically to work over such areas. Indeed, over most forest types, almost full coverage of InSAR observations is possible using this technique (e.g., Gee et al., 2019).

Of particular note is that the ISBAS technique can be used to generate time series of surface motion that capture annual, seasonal, and interseasonal motion of the peat surface (a direct benefit of the improved temporal resolution of Sentinel-1 which acquires data every 6–12 days over the entire land surface of the planet). The characteristics of time series of peatland surface motion are potentially diagnostic of peatland condition (Howie & Hebda, 2018). If InSAR can produce reliable and diagnostic time series over peatland,

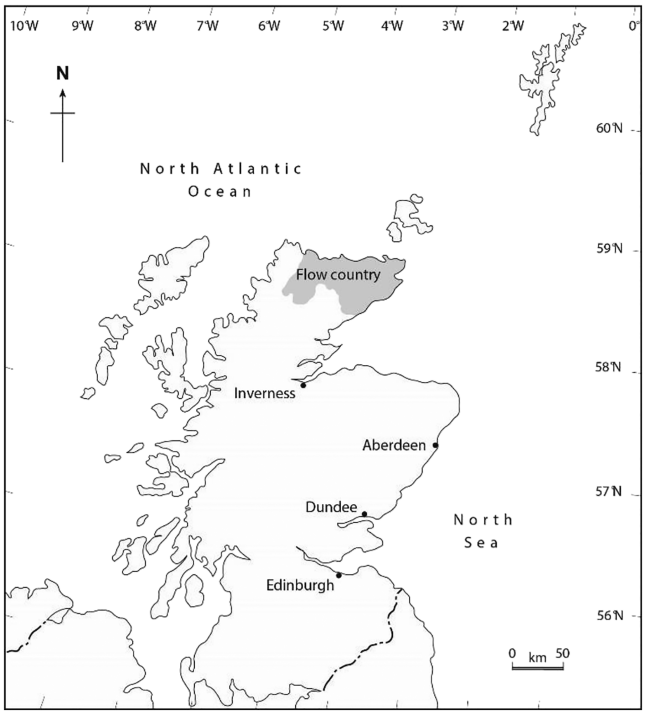


**Figure 1.** Location of the Flow Country in Northern Scotland.

then the technique would enable a new view of peatland surface motion and its relationship to condition and hydrology on a landscape scale and become a powerful tool for landscape scale peatland monitoring across whole catchments, regions, and countries. It must be noted that there is a key barrier to determining the potential of applying InSAR to quantify peatland dynamics and that is the mismatch between the large scale of observation, accuracy, and precision of InSAR and small-scale field observations, which makes it extremely difficult to validate the accuracy of the InSAR results. For example, most published studies depend on transects or single point measures that would be inappropriate to describe the motion of a 80-m × 60-m pixel area as considered in this study. An alternative approach to validating the application of InSAR to quantify peat condition is to abandon concerns of absolute accuracy and focus on whether the characteristics of the InSAR time series can be used to quantify peatland condition, in effect using the InSAR time series as an operationally defined measure, or proxy. The underlying premise that will allow this approach to work is that the InSAR results are representative of the surface motion and that in turn surface motion is representative of peat condition. If attained, this presents an unprecedented view of the peatland.

In this paper, we assess the application of InSAR and the ISBAS method to evaluate peatland condition by applying the ISBAS method to characterize peat motion at high frequencies (via analyses of time series data) over an 21-month period at 22 discrete peatland study sites in the Flow Country, Northern Scotland (Figure 1). Peat condition at each site was determined using plant functional types quantified via field observation, combined with management and land use history data and optical satellite imagery. For each site, the determined peatland condition was compared to the time series data characteristics and the observations evaluated in the context of surface motion, water storage, plant function, and surface energy balance.

## 2. Materials and Methods

### 2.1. Location and Study Site Selection

Twenty-two study sites (Table 1), each cover by two to six ISBAS pixels, were selected in the Flow Country, northern Scotland (centered on 58.371478°N, 3.658447°W—Figure 2a), the largest blanket bog in Europe, to cover a spectrum of peatland conditions. For the purpose of the study, a site is defined as a collection of InSAR pixels found within a peatland forming a mesotope (as defined by Lindsay, 2018). The sites are widely dispersed over a 1,200-km$^2$ area, range in altitudes from 100 to 400 m above sea level and have varied hydrological setting and management histories. Two complementary approaches were taken to site selection: 15 sites were chosen to cover a range of average surface motion (m/year) as had been measured using the ISBAS method over a 21-month period—March 2015 to December 2016 in Alshammari et al. (2018) (Figure 2b) and 7 sites were chosen on account of having existing detailed field measures of peatland condition. Continuous water level data were available for 3 of the 22 sites—where it had been recorded every 30 min along with water temperature with Orpheus mini data loggers.

### 2.2. Site Analysis of Land Cover

For each of the 22 study sites selected for analyses, permission was sought from landowners to undertake vegetation surveys on the ground. Supporting this vegetation survey was a cloud-free Sentinel-2 Multispectral Instrument image. Of these 22 study sites, 12 study sites were visited over a period of 7 days in the peak of the growing season in 2017. At each of those 12 study sites, 4–6 survey locations were randomly selected. At each survey location, a 10-m × 10-m$^2$ was centered on the GPS coordinate of the spatially coincident Sentinel-2 pixel and the four sides of each square were aligned with the cardinal points, thus in the same orientation as the Sentinel-2 pixels. In each of the 10 × 10-m$^2$, the percent cover of key plant functional types (*Sphagnum* mosses, other mosses, lichen, ericaceous shrubs, sedges, grasses, and trees) as well as

**Table 1**
*Site History and Comparison of Site Condition Parameters Derived From Site Visits/Sentinel-2 Optical Imagery (Dominant (>50% Cover) Vegetation Types) and Sentinel-1 ISBAS InSAR Data*

| No. | Study site name | Location OSGB | No. of InSAR pixels | Site description | Dominant vegetation type | InSAR condition parameters | | Peatland condition score |
|---|---|---|---|---|---|---|---|---|
| | | | | | | Mean motion (m/year) | Subsidence class | |
| 1 | Causemire Windfarm | ND1669349095 | 5 | Pool Systems adj. forestry, commercial peat cutting, and wind farm | shrubs and sedges[a] | −0.0100 | High | 2.6 |
| 2 | Smigel Burn | NC9246557048 | 5 | Peat edge adj. natural and man-made drainage | sedges and *Sphagnum*[a] | −0.0080 | High | 2.4 |
| 3 | Wedder Hill | NC9162442992 | 4 | Drained peatland edge adj. stream and drains | shrubgs and sedges[a] | −0.0050 | High | 3.0 |
| 4 | Eileag Burn | NC8360436289 | 4 | Incised peat adj. drains | shrubs and sedges[a] | −0.0040 | Moderate | 3.0 |
| 5 | Cross Lochs | NC8436943685 | 5 | Low disturbance with established pool systems | sedges and *Sphagnum* | 0.0007 | Stable | 2.0 |
| 6 | Blar Geal | ND1016251082 | 4 | Area of pools adj. forestry | *Sphagnum* and sedges[a] | 0.0019 | Stable | 1.3 |
| 7 | Chalybeate Springs | ND1194738116 | 4 | Low disturbance with established pool systems | sedges and *Sphagnum*[a] | 0.0007 | Stable | 1.8 |
| 8 | Cnoc Gleannain | ND0342134141 | 6 | Low disturbance peatland without pool systems | sedges and *Sphagnum*[a] | −0.0020 | Low | 2.3 |
| 9 | Overcaig Hill | ND0324531805 | 6 | Pool system adj. drain | bare peat and shrubs | −0.0040 | Moderate | 3.8 |
| 10 | Strathmore Lodge | ND1123846620 | 4 | Area adj. pool system and historic drainage | sedges and *Sphagnum*[a] | 0.0026 | Stable | 2.1 |
| 11 | Knockfin Heights | NC9256634235 | 4 | Upland, mosaic of pool systems, peat hags, and bare peat | bare peat and shrubs | −0.0050 | High | 4.0 |
| 12 | Munsary Lochans North | ND2173446261 | 4 | Low disturbance with established pool systems | *Sphagnum* and sedges | −0.0012 | Low | 1.0 |
| 13 | Rohan Dubh Lochans | ND2292145525 | 6 | Pool dystem near forestry plantation removed forestry | shrubs and sedges | −0.0033 | Moderate | 2.5 |
| 14 | Munsary Lochans South | ND2271744026 | 4 | Area of former pools adj. historic drainage | sedges and *Sphagnum* | −0.0008 | Low | 1.5 |
| 15 | Loch na Feur | ND2278741728 | 6 | Area adj. forestry plantation and associated drainage | shrubs and sedges | −0.0030 | Moderate | 3.0 |
| 16 | Moss of Whilk | ND2908240479 | 4 | Former forestry and wind farm development | brash | −0.0056 | High | 5.0 |
| 17 | Loch Talaheel | NC9479448635 | 6 | Forest-bog restoration, drain-blocking | shrubs, brash, and grasses | −0.0063 | High | 2.7 |
| 18 | Loch Sletil | NC9683745922 | 4 | Former forested peatland - forest-bog restoration | sedge, brash, and *Sphagnum* | −0.0054 | High | 1.8 |
| 19 | Fountains Dyke | NC8524844304 | 6 | Pool systems immediately adjacent to forestry | *Sphagnum* and sedges | −0.0010 | Low | 1.2 |
| 20 | Loch Caluim | ND0132552946 | 6 | Dry peatland adj. natural drainage | shrubs and sedges | −0.0046 | Moderate | 2.8 |
| 21 | Forsinain/ Dyke | NC8907446472 | 2 | Forested peatland and associated drainage | Conifers and needle litter[a] | −0.0048 | Moderate | 6.0 |
| 22 | Backlass Moss | ND1971353032 | 4 | Drained formerly forested peatland | brash and shrubs[a] | −0.0056 | High | 3.0 |

[a]Sites for which in situ vegetation surveys were not possible due to access restriction. There, local knowledge and Sentinel-2 surveys were used to derive dominant vegetation. Brash refers to coniferous branches and needles left over from forestry removal management activies. Water level data were only available for three sites (Sites 12, 14, and 15). Condition categories were defined using the Braun-Blanquet Scale (Poore, 1955) and are described in section 2.3. No. of InSAR pixels refers to the number of ISBAS pixels (each 4,800 $m^2$) comprising each site (in total 103 ISBAS pixels distributed across the 22 study sites).

key features associated with peatland condition and with the potential to influence the spectral signature of the Sentinel-2 data (bare peat, open water, and vegetation litter/brash) were noted. For each functional group identified, dominant species were also noted. Each square was photographed from the southeast corner, facing north and vegetation patterns reflecting density and spread of dominant plant functional

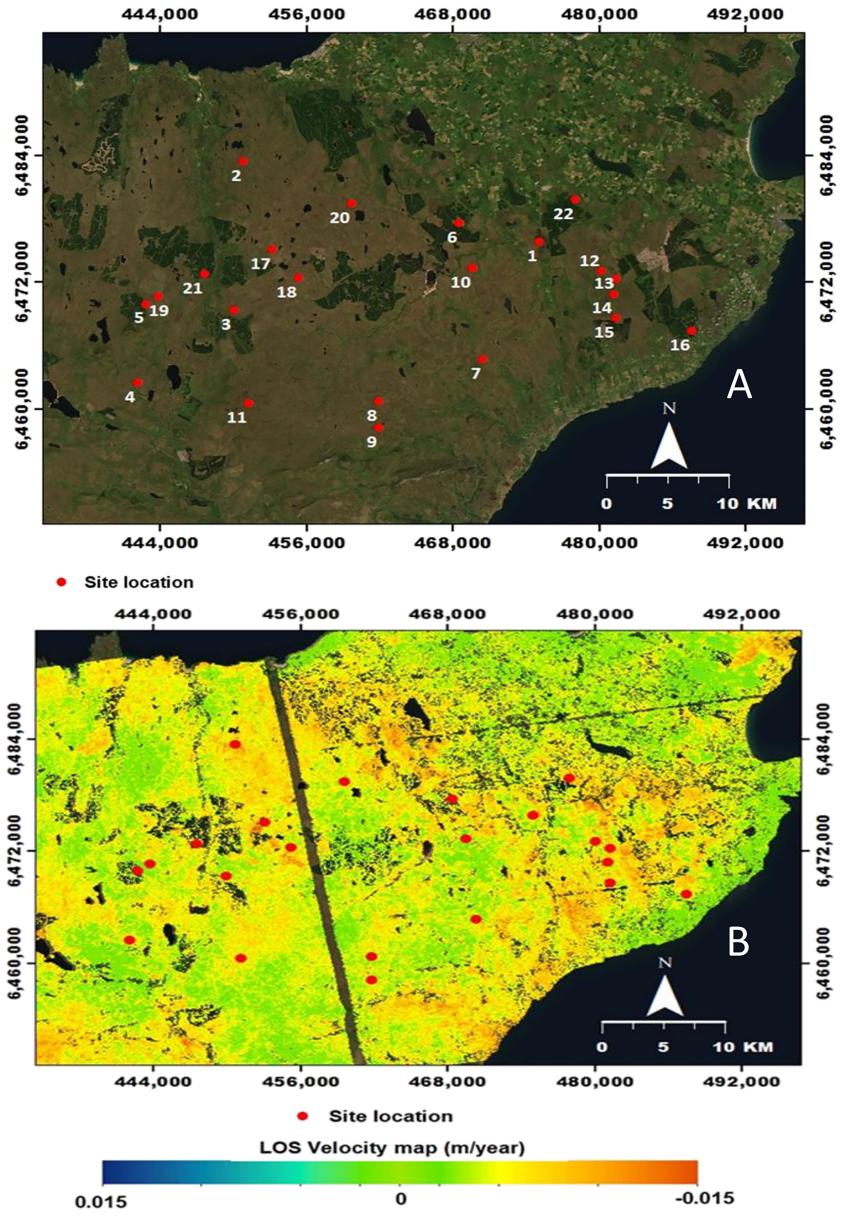


**Figure 2.** (a) Spatial distribution of the 22 study sites within the Flow Country along with (b) the line-of-sight velocity map from ISBAS processing using Sentinel-1 data for the period (March 2015 to November 2016—as per Alshammari et al., 2018). Projection: WGS_1984_UTM_Zone 30. Note negative values correspond to subsidence, that is, moving away from the sensor and vice versa.

groups were drawn and annotated for future reference. For each site, general condition was further assessed by noting the presence of drains, tracks, evidence of deer trampling or browsing, presence of natural pools, restoration activity, and estimating distance to road, forestry or infrastructure within a 100-m × 100-m area around the groups of squares. Land use history was documented by discussion with land owners.

For 10 survey sites access was not possible during the survey period, but all had been previously visited for other projects by one of the authors, or by land managers. Using this information and that obtained from surveys of the 12 study sites that had been visited, the remaining 10 study sites were characterized via a classification of the afore-mentioned Sentinel-2 Multispectral Instrument optical satellite image (dated from September 2015; downloaded from earthexplorer.usgs.gov and preprocessed using the Sentinel-2 toolbox from European Space Agency to resample all wavebands to 10-m spatial resolution). A series of land cover classifications were conducted, with pixels covering the 10 inaccessible study sites allocated to one of the

following classes: water, *Sphagnum*, sedges, shrubs, bare peat, grass, trees, and brash. The classifiers used were (i) support vector machine, (ii) spectral angle mapper, and (iii) spectral information divergence (Mather & Koch, 2011; Mathur & Foody, 2008), and the resultant classified pixels for the 10 remaining sites were determined by way of an ensemble decision rule (Foody et al., 2007). Given that these sites were inaccessible an accuracy assessment was not possible hence the use of an ensemble approach. The dominant (most frequently occurring) land covers allocated to the Sentinel-2 pixels across each of the 10 sites were noted. This combination of detailed field observations and spectral discrimination of the Sentinel-2 imagery afforded the determination of the peatland condition (see section 2.3) of each of the 22 study sites used in the subsequent analyses.

### 2.3. Determination of Peatland Condition

All the information on each study site was put together, and, supported by the literature, condition categories were established that represent a gradation in peatland condition using the Braun-blanquet scale (Poore, 1955). Typical conditions are illustrated in Figure 3. Condition 1 represents what is generally considered to be wet peatland in good condition with a shallow water table (<10 cm below peat surface) with high *Sphagnum* moss cover (≥50%) growing in large continuous carpets and high cover of sedges (also ≥50%, largely dominated by *Eriophorum angustifolium* and *Tricophorum germanicum*), with some shrubs (mostly *Erica tetralix*). Condition 2 represents wet peatland in relatively good condition with some patches of *Sphagnum* mosses (25–50%) and sedges (25–75%), but signs of disturbance or lower water table, for example, increased shrubs, particularly *Calluna vulgaris* and lichen, small patches of bare peat, or evidence of deer activity. Condition 3 represents degraded peatland sites with small clumps of *Sphagnum* mosses (10–25%) often including species associated with disturbance (e.g., *S. tenellum* and *S. fallax*), high sedge cover (20–75%) combined with shrub and lichen dominance, presence of grasses (e.g., *Molinia caerulea* and *Deschampsia flexuosa*) and indication of disturbance at the wider scale, for example, drainage ditches, areas of bare peat (10–25%), deer trampling or known past disturbance (hill drains, grazing, fire). Condition 4 is generally considered to be highly degraded peatland in poor condition with a deep water table (typically >15 cm below surface and with sustained periods >20 cm) evidenced by large areas of bare peat (>25%), a predominance of shrubs almost exclusively *C. vulgaris* fewer sedges and less than 10% *Sphagnum* confined to small isolated clumps, also including clear disturbance both within the squares and in the wider area. Condition 5 defines clear-felled conifer plantation on peat that displays typical linear features associated with past furrows and plow through and has high cover of brash. Condition 6 defines commercial conifer plantation on peatland, with dense cover of *Pinus contorta* and *Picea sitkensis* and understorey characterized by needle litter, no *Sphagnum* and sparse cover of forest mosses. Using these condition categories, Conditions 1–6 were attributed to each ISBAS pixel within a site (Figures 3 and 4) and an average condition score calculated for each site based on the average of the attributed condition value (1–6) (Table 1).

### 2.4. InSAR Processing and the ISBAS Method

The ISBAS method is a coherent pixel technique and is a novel variant of the Small Baseline Subset method (Berardino et al., 2002). The main novelty lies in the abandonment of the requirement for consistent phase stability in all observations, which is a requirement for most time series InSAR methods (Hooper et al., 2012). It has been fully validated through comparisons with leveling (Gee et al., 2016) and over urban areas, which demonstrated that standard errors of less than 2 mm/year are possible. Although, in terms of time series, there is a increased level of noise in rural areas, which may be due to a decrease in observations due to intermittent coherence but also may reflect the naturally high variations of a natural surface, ISBAS results fully agree with subsidence characteristics from other InSAR surveys, such as PSInSAR (Gee et al., 2017; Sowter et al., 2016). The method has been shown to detect subsidence and uplift features associated with underground mining under agricultural and forested areas (Bateson et al., 2015; Gee et al., 2017; Sowter et al., 2013). More recently, the ISBAS method has been shown to give near complete land area coverage over peatland areas (Alshammari et al., 2018; Cigna & Sowter, 2017).

The analysis here used freely available Sentinel-1 C-band SAR data from the European Space Agency's Copernicus Open Access Hub [scihub.copernicus.eu] that covered a 21-month period from March 2015 to December 2017. The Sentinel-1 mission is part of the European Union's Copernicus Programme, which plans to regularly gather environmental data over the entire globe for the foreseeable future. Rates of motion and time series are generated relative to selected stable reference points. In this study the stable reference

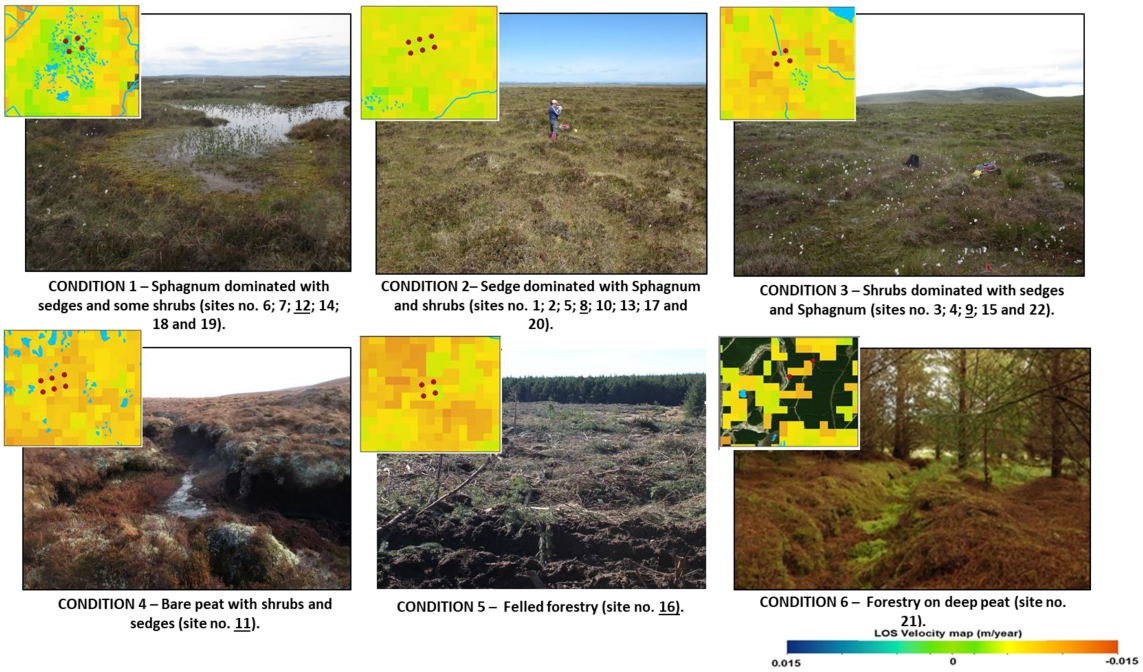


**Figure 3.** Photographic data illustrating an example site for each of the six peatland conditions. For each condition type an extract of the ISBAS surface motion output (m/year) is presented with the red dots representing the ISBAS pixels used in subsequent analyses (as listed in Table 1); the site used for illustration stated in the caption.

point used is located at Dounreay on the north coast at 58°34′37.9″N, 03°44′10.4″W (following Alshammari et al., 2018). ISBAS InSAR processing used a temporal baseline of 21 months and a normal perpendicular baseline of 200 m. A map of the images and pairs used provided (supporting information Figure S2). The work of Cigna et al. (2014) points out that the standard error is dependent on the number of coherent layers used. Although Sentinel-1 data used was across a 21-month period, there were 47 images acquired, forming 1,071interferograms. This implies a high redundancy and, therefore, good precision of better than 2 mm in this case. Processing of these outputs will then provide two InSAR motion data sets for each ISBAS pixel (an ~80-m × 60-m area): the long-term motion trend over the full 21-month period and the subannual variation in surface motion. At most of the study sites (Table 1 and Figure 2) the data sets were extracted from four to six ISBAS pixels the only exception being the forested site, which was covered by only two ISBAS pixels.

The use of long temporal baselines, in this case up to 21 months, is important in the identification of more subtle deformation trends. Over vegetated and natural surfaces, it may be anticipated that long baseline pairs contain no useful velocity information as InSAR requires invariant phase conditions to maintain phase coherence. Practical demonstrations of this over permafrost areas in the summer period (e.g., Liu et al., 2010) have shown that, on the contrary, good phase measurements are possible when using pairs from

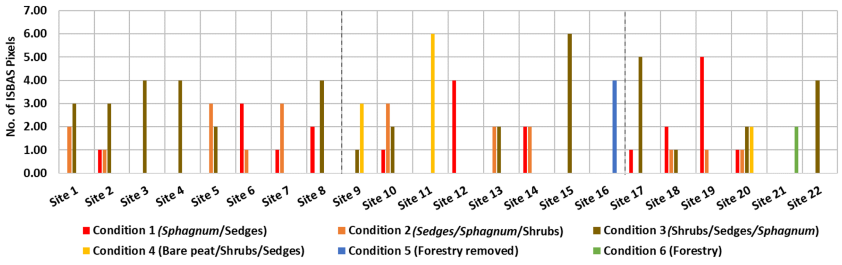


**Figure 4.** Histogram illustrating range of conditions encountered on each site. Frequency refers to the number of 60 × 80-$m^2$ ISBAS pixels in a particular condition category on each site.

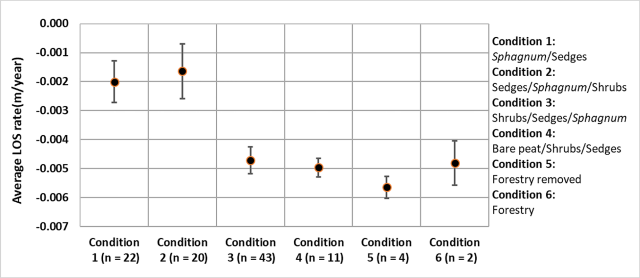


**Figure 5.** Comparison of the average line-of-sight (LOS) velocity versus peat condition category. Mean LOS velocity is the mean velocity of all ISBAS pixels (*n*) in each condition category The error bars represent the standard error of the mean of LOS velocity under each condition category.

season-to-season and over a number of years. For this reason, we do not restrict the analysis to short pairs only.

It will be noted that the ISBAS coverage over the forested areas was not complete in some cases. As mentioned above, the ISBAS method allows measurement of intermittently coherent pixels but only if the pixel is coherent in enough interferograms to meet an arbitrary threshold. Forests can be particularly challenging in this respect and, although coverage was generally excellent, some pixels did not meet this criteria and are excluded from the survey.

### 2.5. Time Series Processing of the ISBAS InSAR Outputs

The displacement time series was extracted from the ISBAS InSAR outputs as per section 2.4, using a method identical to that used in Small Baseline Subset data processing (Berardino et al., 2002). This involves the adjustment of the InSAR pairs to derive the displacement at each observation date and then filtering to remove the atmospheric phase screen. Trends in the short time series were extracted using singular spectrum analysis and Kendalls Tau nonparametric trend test in the SSA-MTM toolkit (Dettinger et al., 1995; Ghil et al., 2002). Seasonal timing of peaks and troughs was determined from the position of maxima and minima in trends from which the long-term linear component had been removed. To enable a more effective comparison between the InSAR time series and water level time series, normalization was applied by subtracting the mean and dividing by the standard deviation. Where normalization is applied this is stated in the figure caption.

In presenting and referring to the InSAR data the convention used throughout this paper is that subsidence, that is, displacements moving away from the satellite sensor are shown as negative values and vice versa.

## 3. Results

### 3.1. Peatland Condition and Associated Surface Motion

From the collated study site information (Table 1 and Figures 3 and 4) it is evident that all peatland condition categories (1 to 6) are present within the sample. Comparison of the average line-of-sight surface velocities (m/year) for ISBAS pixels in each condition class (Figure 5) illustrates that *Sphagnum*-deficient conditions (i.e., Conditions 3–6) have significantly higher rates of subsidence than *Sphagnum*-rich conditions (Conditions 1 and 2).

### 3.2. Characterization of Peatland Behavior: Outputs From Time Series Processing

Based on the similarity of the trends extracted using singular spectrum analysis, the InSAR time series of surface motion for each of the 22 study sites were seen to group into four categories labeled Categories A to D (Figure 6). Category A sites display distinct high amplitude seasonal oscillations (Figure 6a); Category B sites also display distinctly low amplitude seasonal oscillations (Figure 6b); Category C sites display a subsidence trend with little or no seasonal oscillation (Figure 6c); and Site 18 (Figure 6d) does not fit into any of the Categories A to C and displays both high rates of subsidence and peak uplift during the year (November–December) and thus been allocated to Category D. Category A shows a clear uplift trend that is not indicated in the average velocity maps. However, the uplift trend is actually very small, with a rate of only around 2 mm/year on average, and simply too small to show up on the color ramp used which runs between ±15mm/year.

Using only sites covered by ISBAS pixels in Condition Categories 1 to 4 an average condition score was calculated for each of the Categories A to D (Table 2). Average condition scores were not calculated for the Forestry Sites 21 and 16 as these did not contain vegetation that is part of the natural continuum in plant functional type. Category A sites have an average condition score of 1.64 and predominantly contain ISBAS pixels in Conditions 1 and 2, and thus, Category A is associated with good peatland condition. Category B sites have an average condition score of 2.89 and contain the broadest mix of conditions but are predominantly covered by ISBAS pixels in Conditions 2 and 3, both good and poor peatland. Category C sites have an average condition score of 2.96 and are dominated by Condition 3 (and one site that falls

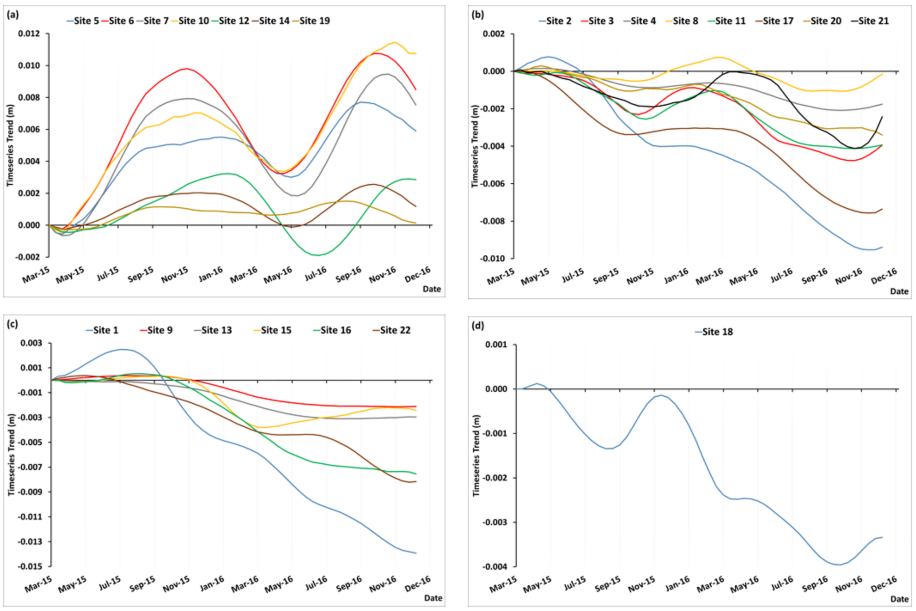


**Figure 6.** InSAR time series trends from the 22 sites grouped by Categories A (a), B (b), C (c), and D (d).

under Condition 5—Study Site 16 which is a former forested site). Forested sites lie in Category B (Site 21) and clear felled forest sites in Categories C (Site 16) and D (Site 18). In this distribution of sites between peatland condition and category it is evident that the presence/absence of *Sphagnum* is a key determinant of good peatland condition.

The timings of seasonal peaks and troughs in the time series for study sites in Categories A and B are different (Figure 7). Category A sites display a distinctly higher amplitude seasonal oscillations with peak subsidence in April–June and peak uplift in August–November, whereas Category B sites display distinct low amplitude seasonal oscillations with peak subsidence in July–October and peak uplift in February–June.

Comparison of normalized InSAR surface motion and water level (Figure 8) for Sites 12, 14, and 15 indicate that, for the *Sphagnum*-dominated Sites 12 and 14 (InSAR Category A, Conditions 1+2), there is notable coherence between the InSAR seasonal trends and some coherence in the interseasonal oscillations. For Site 15, the only site with drainage and signs of degradation (InSAR Category C, Condition 3), interseasonal oscillations appear to be out of phase and the InSAR time series does not display a seasonal trend.

## 4. Discussion

The peatlands of the Flow Country in northern Scotland have been examined in a novel and unprecedented way by virtue of the recent availability of Sentinel-1 SAR data and the development of the ISBAS technique (Sowter et al., 2016). Building on earlier studies (Alshammari et al., 2018; Cigna & Sowter, 2017), which demonstrated the potential of using InSAR for surface motion measurements in peatland, peatland surface motion was measured at high temporal frequencies, at unprecedented spatial resolutions, and demonstrated to be linked with peatland condition. Sites in good condition (wet, *Sphagnum* dominated, often with pool systems) display markedly different long-term and seasonal surface motion trends in comparison to shrub-dominated sites associated with poorer condition over the same period. Furthermore, although limited to three sites, comparison of surface oscillations measured by InSAR to water level indicates that for wet sites in good condition the two are strongly related and track each other, an observation that is consistent with other field observations that indicate peatland surface motion tracks changes in water level (Fritz et al., 2008; Reeve et al., 2013).

It would seem to be the case that the InSAR-derived surface motion time series provide a measure of the mechanical movement of the surface as it responds to changing water storage within the peat. By applying this explanation, the InSAR-derived surface motion time series can be thought of as being composed of long-

**Table 2**
*Conditions Associated With Each Time Series Category*

| | | Sites in category | Average condition score | Number of ISBAS pixels in a particular condition associated with the each time series category | | | | | |
|---|---|---|---|---|---|---|---|---|---|
| | | | | Condition category | | | | | |
| | | | | 1 | 2 | 3 | 4 | 5 | 6 |
| Time series Category | A | 5,6,7,10, 12,14,19 | 1.64 | 16 | 13 | 4 | 0 | 0 | 0 |
| | B | 2,3,4,8, 11,17,20, **21** | 2.89 | 5 | 2 | 22 | 8 | 0 | 2 |
| | C | 1,13,9,15,**16,** 22 | 2.96 | 0 | 4 | 16 | 3 | 4 | 0 |
| | D | 18 | 1.75 | 2 | 1 | 1 | 0 | 0 | 0 |

*Note*. Average condition score is the average condition of an ISBAS pixel in each time series category and is calculated by assigning Values 1–4 to Condition Categories 1–4. Number of ISBAS pixels in each category is also presented and is derived from the site data presented in Figure 4. Note that Condition Categories 5 and 6 corresponding to Forested Sites 21 and 16 (in bold) were not used in the calculation of the average condition score.

term unidirectional changes in the mass of organic matter and water stored in the peat and short-term reversible seasonal or higher frequency oscillations in response to drying and wetting (Camporese et al., 2006). The presence of seasonal oscillations indicates a direct link between the mechanical motion, water storage, and surface energy balance of the peatland (Lafleur et al., 2005), and it is in this context that the mechanisms linking peatland condition to the characteristics of the InSAR-derived surface motion time series will be discussed.

Of the 22 study sites under analysis those labeled as Category A by virtue of their InSAR-derived surface motion were *Sphagnum* and sedge dominated with a shallow, near-surface water table and most harbor extensive pool systems. Evaporation through *Sphagnum* is directly linked to the evaporative demand of the atmosphere and depth to water table. The high-amplitude seasonal cycles and midsummer/midwinter seasonal minima and maxima are therefore most likely due to the seasonal influence of evaporative demand on water loss through *Sphagnum* species (Lapen et al., 2000). In terms of latent heat flux ($Q_E$) partitioning, the maximum partitioning to *Sphagnum* occurs at the time of minimum leaf area index in late April to early May when moss is at its wettest and before the peak $Q_E$ in vascular systems (Admiral & Lafleur, 2007). Maximum drawdown of *Sphagnum* surfaces should therefore precede vascular surfaces. The surface motion of *Sphagnum* bogs is also considered a self-preservation mechanism (Golubev & Whittington, 2018). As water is lost in response to increased evaporative demand the surface elevation drops, maintaining a relatively constant and essential supply of moisture to the *Sphagnum* surface (Golubev & Whittington, 2018; Lafleur & Roulet, 1992). If the water level continues to fall water transfer through *Sphagnum* becomes increasingly difficult and water loss through the surface becomes negligible (Kettridge et al., 2016; Lafleur & Roulet, 1992), effectively acting as a negative feedback that acts to constrain the later growing season drawdown of the *Sphagnum* surface. The physiology of *Sphagnum* therefore shifts maximum drawdown

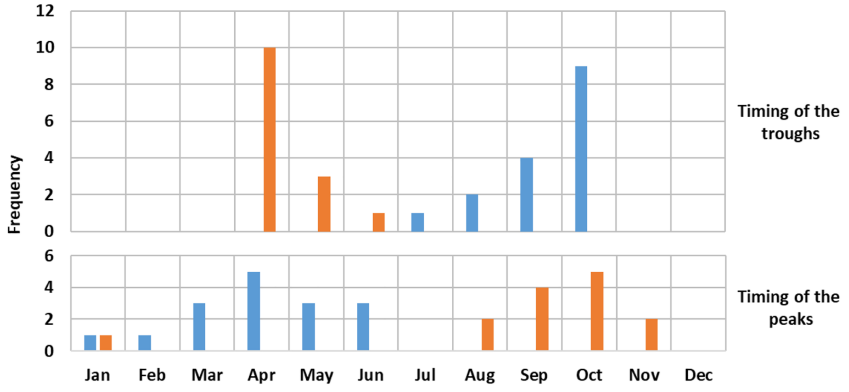


**Figure 7.** Histogram showing the frequency and timing of the troughs and peaks in time series Categories A (in Orange) and B (in Blue).

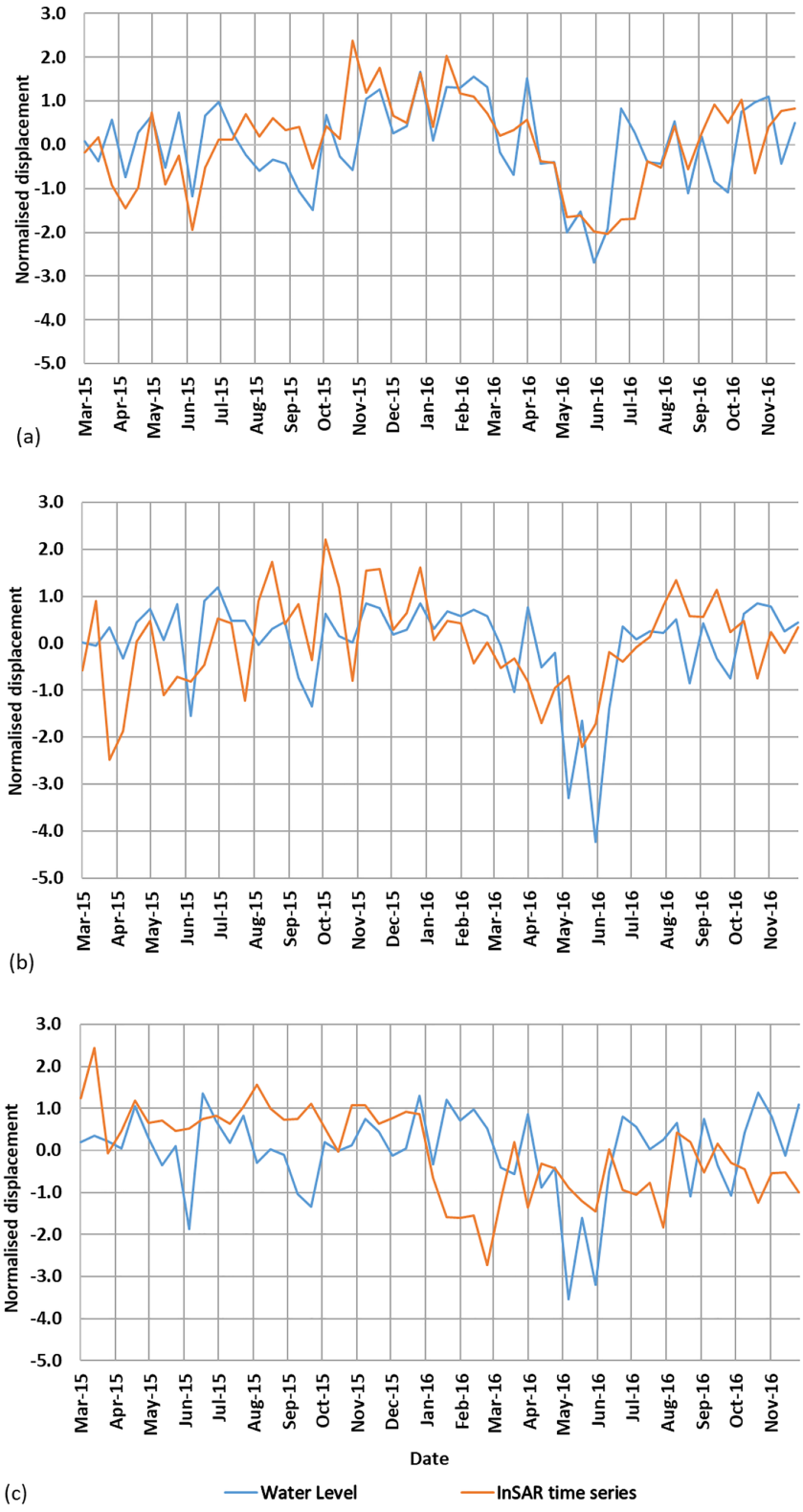


**Figure 8.** Comparison of water level to InSAR time series. Both the surface motion and water level have been normalized relative to the mean and standard deviation. (a) Site 12 is a Category A site with a condition score of 1, and the result water level is the average of two closely spaced piezometers, one in a hollow at OSGB coordinates ND 21761 46322 and the other on a low ridge at ND 21767 46318. (b) Site 14 is a Category A site with average condition score of 1.5, position of the piezometer is on a low ridge at OSGB coordinates ND 22974 45573. (c) Site 15 is a Category C site with average condition score of 3, positions of the piezometer is on a low ridge at OSGB coordinates ND 22746 44079.

and recharge of the water table and associated surface motion to a midsummer/midwinter pattern that aligns with seasonal variations in evaporative demand in the United Kingdom (Robinson et al., 2017).

Category B sites are interpreted as degraded but not as severely degraded as Category C sites. These sites include a greater mixture of plant functional types, are dominated by vascular plants but do include some areas of *Sphagnum*, and are interpreted to be generally wetter with a greater capacity for seasonal water storage. Unlike Category C sites, the seasonal oscillations are distinct but generally of lower amplitude than those observed in Category A sites. This is interpreted as indicating that the water table is shallower than at Category C sites and deeper than at Category A sites with variations occurring within a less degraded peat with greater porosity, elasticity, and specific storage than the Category C sites. The predominance of deeper rooted vascular plants that exercise a strong seasonal evapotranspiration drawdown on water level throughout the growing season may explain why water levels reach a minimum at the end of the growing season in late summer/early autumn and recover to a maximum ahead of the growing season in late winter/early spring (Bourgault et al., 2017). This interpretation is supported by studies of $Q_E$ partitioning, which indicate that the $Q_E$ from vascular plants peaks when leaf area is at its maximum in June–July and stays high until senescence in the late growing season (Admiral & Lafleur, 2007).

Category C sites are degraded due to drainage, display sustained subsidence, contain little or no *Sphagnum*, and lack seasonal oscillations. The lack of seasonal oscillation probably results from several factors associated with peat degradation. Loss of compressibility and a reduced response to changes in effective pressure within the peat is an irreversible consequence of enhanced decay at the more degraded sites (Kennedy & Price, 2005; Waddington & McNeill, 2002). A lack of responsiveness to changes in surface energy (via both evaporative demand and evapotranspiration) is due to a deep falling water table and water storage below root depth (Lafleur et al., 2005) imposing a mass transfer limitation on water loss by evapotranspiration (Schwarzel et al., 2006). Low permeability and porosity of the compacted, humified, inelastic peat combined with the possible presence of fracture porosity because of shrinkage does not permit significant water storage within the peat matrix.

The distinctiveness of the Category D, Site 18 (Figure 6d), which displays surface motion characteristics that are a mixture of Category A and Category C, is interpreted as being indicative of site management specifically: Following two decades under forestry management (conifer plantation), the site was felled (trees and brash left on site, rolled into the furrows dug for forestry) and drains were blocked in 2003–2004, with further blocking of furrows and brash crushing to smoothen the surface completed in 2016–2017. The Category C component is interpreted as evidence of shallow water table and probable colonization by *Sphagnum* in areas of ditch blocking. The strong subsidence component more typical of Category C sites could indicate that despite rewetting the site is still losing mass, which is consistent with observations (Hambley, 2016) or could be in part due to compaction by heavy machinery during the final phase of restoration in 2016–2017. It is also notable that this contrasts with Site 17, another forest to bog restoration site, which was restored in 1998 which, although drier and dominated by shrub vegetation, displays surface motion trends that lie within Category B and is a net carbon sink (Hambley, 2016).

The step change in the InSAR characteristics between wet, *Sphagnum*-rich sites in good condition and sites with a deeper water table in poorer condition has the potential to provide a threshold for characterizing peatland condition. A similar step change has been noted with respect to the evapotranspiration behavior in Ontario peatlands (Lafleur et al., 2005) with evapotranspiration declining markedly when the water table depth drops more than 60 cm below hummock top. Similarly, a water table depth threshold of 35 cm has been reported for reduction in evapotranspiration through mosses (Mezbahuddin et al., 2016). In both instances the step change occurs when mass transfer limits water loss by evaporation or evapotranspiration. To account for the relationship between evapotranspiration, plant functional type, and water table depth, Lafleur et al. (2005) proposed the following three-stage conceptual model. At sites with a shallow water table (<30 cm) *Sphagnum* dominates and loss of water by evaporation is not significantly limited mass transfer. As the water table falls to depths of between 30 and 60 cm shallow rooted vascular plants increasingly dominate the evapotranspiration. As the water table falls below the maximum rooting depth of the vascular plants there is a step change when the mass transfer of water to plant roots becomes the predominant factor controlling rates of evapotranspiration rather than the evaporative demand. In many ways, this is remarkably similar to the interpretation given above with the exception that the three-stage model proposed by

Lafleur et al. (2005) addresses the evapotranspiration trends over a season at a single site and not the variation between sites. It is also similar to the observations of Schwarzel et al. (2006) who noted that in dry years evapotranspiration is limited by mass transport in the soil, whereas in wet years evapotranspiration is mostly controlled by evaporative demand. Mechanisms that underpin the model of Lafleur et al. (2005) and the conclusions of Schwarzel et al. (2006) should be equally applicable to sites in different condition. Sites experiencing long-term drainage and water loss behave in a manner that is equivalent to the water table falling below the maximum rooting depth. A step change, due to a shift in the processes controlling mass transfer, occurs between the wet, growing, *Sphagnum* dominant sites and those with a long-term falling water table.

## 5. Conclusions

The interpretation presented carries important implications: Surface motion attributed to changes in water budget, water table depth, and energy balance are also linked to carbon balance and net ecosystem exchange (Laine et al., 2007; Mezbahuddin et al., 2017; Moore et al., 1998). Hence, if the InSAR time series capture meaningful characteristics of the surface motion, this will open up a new view of peatland dynamics on an unprecedented scale that could not be practically achieved using standard field-based techniques. As changes in water storage due to drainage or restoration should precede ecological change, InSAR time series characteristics also have the potential to offer a sensitive monitoring tool that can be used to quantify evolving peatland condition. InSAR measure of surface motion could also be used to assess nonuniformity of biogenic gas buildup (Comas et al., 2005; Reeve et al., 2013) and investigate natural peatland successions, for example, the postulated shift from hollow to hummock as bog elevation grows and species that tolerate drier hummock conditions outcompete species that prefer wetter conditions (Robroek et al., 2007). The use of InSAR time series should enable a new approach to regional peatland monitoring through the application of time series analysis techniques more typically deployed in climatology and oceanography (e.g., principal component analysis and extended empirical orthogonal functions). In turn, this approach may enable a range of regional-scale scientific questions to be addressed with respect to coupling between peat, landscape and climate.

The InSAR measurements using the ISBAS method has resulted in remarkable coverage over a vegetated region, something not usually anticipated when using a C-band sensor. However, this has not been without cost as the spatial resolution of the raw Sentinel-1 data, around 14 m × 3 m, has had to be degraded in order to reduce phase noise. Accuracy also improves with the number of observations (Cigna & Sowter, 2017), and we would not anticipate good results if less than, say, 30 images were available over a site, which may limit the capability to utilize archive satellite data from, for example, the ENVISAT and ERS missions. The method may also benefit from a longer wavelength, such as L-band, which has an improved capability to measure the larger rates that characterize peat motion in other regions, such as the tropics.

Finally, what we have considered is the empirical relationship between the InSAR measures and the site condition. We have not assessed the accuracy of the InSAR measurement. There is also a question as to the representativeness of the InSAR signal and in particular whether different parts of the peat surface, for example, hummocks and hollows, contribute equally to the InSAR measurement. By addressing these questions, a far greater understanding of the radar response may be obtained. To achieve a true assessment of accuracy will be difficult, as single points or short transects do not replicate the totality of the InSAR measurement obtained using the ISBAS method and where peatland field data are available the error in field measurements is a major source of uncertainty. However, despite this validation difficulty the precision of the measurement is sufficient to produce a meaningful signal that relates to peatland processes and condition. The results of this study could be used to underpin a satellite-based monitoring system based on C-band SAR images that could operate over peatlands monitoring their condition at unprecedented scales.

**Acknowledgments**

The authors are unaware of any real or perceived conflicts of interests either financial or by affiliation. L. A. acknowledges the financial support of the Higher Education and Scientific Research Ministry in Iraq for the PhD scholarship (and directed by D. B. and S. M.). Rahman Momeni is thanked for assistance with field work and data processing. We are grateful to the Royal Society for the Protection of Birds (RSPB), Plantlife Scotland, Wellbeck Estate, Shurrery estate, and Forestry and Land Scotland for granting us access to sites for vegetation surveys. Data used in this paper are available online (http://doi.org/10.17639/nott.7029). A. S., C. M., P. G., D. J. L., and R. A. acknowledge support from NERC Grant NE/P014100/1.

## References

Admiral, S. W., & Lafleur, P. M. (2007). Modelling of latent heat partitioning at a bog peatland. *Agricultural and Forest Meteorology*, *144*(3-4), 213–229. https://doi.org/10.1016/j.agrformet.2007.02.005

Alshammari, L., Large, D. J., Boyd, D. S., Sowter, A., Anderson, R., Andersen, R., & Marsh, S. (2018). Long-term peatland condition assessment via surface motion monitoring using the ISBAS DInSAR technique over the flow country, Scotland. *Remote Sensing*, *10*(7), 1103. https://doi.org/10.3390/rs10071103

Bateson, L., Cigna, F., Boon, D., & Sowter, A. (2015). The application of the Intermittent SBAS (ISBAS) InSAR method to the South Wales Coalfield, UK. *International Journal of Applied Earth Observation*, *34*, 249–257. https://doi.org/10.1016/j.jag.2014.08.018

Berardino, P., Fornaro, G., Lanari, R., & Sansosti, E. (2002). A new algorithm for surface deformation monitoring based on small baseline differential SAR interferograms. *Ieee T Geoscience Remote*, *40*(11), 2375–2383. https://doi.org/10.1109/Tgrs.2002.803792

Bourgault, M. A., Larocque, M., & Garneau, M. (2017). Quantification of peatland water storage capacity using the water table fluctuation method. *Hydrological Processes*, *31*(5), 1184–1195. https://doi.org/10.1002/hyp.11116

Camporese, M., Ferraris, S., Putti, M., Salandin, P., & Teatini, P. (2006). Hydrological modeling in swelling/shrinking peat soils. *Water Resources Research*, *42*, W06420. https://doi.org/10.1029/2005wr004495

Cigna, F., & Sowter, A. (2017). The relationship between intermittent coherence and precision of ISBAS InSAR ground motion velocities: ERS-1/2 case studies in the UK. *Remote Sensing of Environment*, *202*, 177–198. https://doi.org/10.1016/j.rse.2017.05.016

Cigna, F., A. Sowter, C. J. Jordan, and B. G. Rawlins (2014), Intermittent Small Baseline Subset (ISBAS) monitoring of land covers unfavourable for conventional C-band InSAR: Proof-of-concept for peatland environments in north Wales, UK, Proc Spie, 9243, doi:https://doi.org/10.1117/12.2067604.

Comas, X., Slater, L., & Reeve, A. (2005). Geophysical and hydrological evaluation of two bog complexes in a northern peatland: Implications for the distribution of biogenic gases at the basin scale. *Global Biogeochemical Cycles*, *19*, GB4023. https://doi.org/10.1016/j.jhydrol.2005.04.020

Dettinger, M. D., Ghil, M., Strong, C. M., Weibel, W., & Yiou, P. (1995). Software expedites singular-spectrum analysis of noisy time series. *Eos, Transactions of the American Geophysical Union*, *76*(2), 12–21. https://doi.org/10.1029/EO076i002p00012

Even, M., & Schultz, K. (2018). InSAR deformation analysis with distributed scatterers: A review complemented by new advances. *Remote Sensing*, *10*, 744. https://doi.org/10.3390/rs10050744

Ferretti, A., Prati, C., & Rocca, F. (2000). Nonlinear subsidence rate estimation using permanent scatterers in differential SAR interferometry. *IEEE Transactions on Geoscience and Remote Sensing*, *38*(5), 2202–2212. https://doi.org/10.1109/36.868878

Ferretti, A., Prati, C., & Rocca, F. (2001). Permanent scatterers in SAR interferometry. *IEEE Transactions on Geoscience and Remote Sensing*, *39*(1), 8–20. https://doi.org/10.1109/36.898661

Fiaschi, S., Holohan, E. P., Sheehy, M., & Floris, M. (2019). PS-InSAR Analysis of Sentinel-1 data for detecting ground motion in temperate oceanic climate zones: A case study in the Republic of Ireland. *Remote Sensing*, *11*, 348. https://doi.org/10.3390/rs11030348

Foody, G. M., Boyd, D. S., & Sanchez-Hernandez, C. (2007). Mapping a specific class with an ensemble of classifiers. *International Journal of Remote Sensing*, *28*(7-8), 1733–1746. https://doi.org/10.1080/01431160600962566

Fritz, C., Campbell, D. I., & Schipper, L. A. (2008). Oscillating peat surface levels in a restiad peatland, New Zealand—Magnitude and spatiotemporal variability. *Hydrological Processes*, *22*(17), 3264–3274. https://doi.org/10.1002/hyp.6912

Gee, D., Bateson, L., Sowter, A., Grebby, S., Novellino, A., Cigna, F., et al. (2017). Ground motion in areas of abandoned mining: Application of the Intermittent SBAS (ISBAS) to the Northumberland and Durham Coalfield, UK. *Geosciences*, *7*, 85. https://doi.org/10.3390/geosciences7030085

Gee, D., Sowter, A., Grebby, S., de Lange, G., Athab, A., & Marsh, S. (2019). National geohazards mapping in Europe: Interferometric analysis of the Netherlands. *Engineering Geology*, *256*, 1–22. https://doi.org/10.1016/j.enggeo.2019.02

Gee, D., Sowter, A., Novellino, A., Marsh, S., & Gluyas, J. (2016). Monitoring land motion due to natural gas extraction: Validation of the Intermittent SBAS (ISBAS) DInSAR algorithm over gas fields of North Holland, the Netherlands. *Marine and Petroleum Geology*, *77*, 1338–1354. https://doi.org/10.1016/j.marpetgeo.2016.08.014

Ghil, M., Allen, M. R., Dettinger, M. D., Ide, K., Kondrashov, D., Mann, M. E., et al. (2002). Advanced spectral methods for climatic time series. *Reviews of Geophysics*, *40*, 1003. https://doi.org/10.1029/2000RG000092

Glenk, K., Schaafsma, M., Moxey, A., Martin-Ortega, J., & Hanley, N. (2014). A framework for valuing spatially targeted peatland restoration ecosystem services. *Ecosystem Services*, *9*, 20–33. https://doi.org/10.1016/j.ecoser.2014.02.008

Golubev, V., & Whittington, P. (2018). Effects of volume change on the unsaturated hydraulic conductivity of *Sphagnum* moss. *Journal of Hydrology*, *559*, 884–894. https://doi.org/10.1016/j.jhydrol.2018.02.083

Grebby, S., Orynbassarova, E., Sowter, A., Gee, D., & Athab, A. (2019). Delineating ground deformation over the Tengiz oil field, Kazakhstan, using the Intermittent SBAS (ISBAS) DInSAR algorithm. *International Journal of Applied Earth Observation and Geoinformation*, *81*, 37–46. https://doi.org/10.1016/j.jag.2019.05.001

Hambley, G. (2016), The effect of forest-to-bog restoration on net ecosystem exchange in The Flow Country peatlands, PhD Thesis 261 pp, University of St Andrews.

Hooper, A., Bekaert, D., Spaans, K., & Arikan, M. (2012). Recent advances in SAR interferometry time series analysis for measuring crustal deformation. *Tectonophysics*, *514*, 1–13. https://doi.org/10.1016/j.tecto.2011.10.013

Howie, S., & Hebda, R. (2018). Bog surface oscillation (mire breathing) a useful measure in raised bog restoration. *Hydrological Processes*, *32*(11), 1518–1530. https://doi.org/10.1002/hyp.11622

Ingram, H. A. P. (1983). Hydrology. In A. J. P. Gore (Ed.), *Ecosystems of the World 4B Mires: Swam, bog, fen and moor—Regional studies* (pp. 67–158). Amsterdam: Elsevier Science.

Kennedy, G. W., & Price, J. S. (2005). A conceptual model of volume-change controls on the hydrology of cutover peats. *Journal of Hydrology*, *302*(1), 13–27. https://doi.org/10.1016/j.jhydrol.2004.06.024

Kettridge, N., Tilak, A. S., Devito, K. J., Petrone, R. M., Mendoza, C. A., & Waddington, J. M. (2016). Moss and peat hydraulic properties are optimized to maximize peatland water use efficiency. *Ecohydrology*, *9*(6), 1039–1051. https://doi.org/10.1002/eco.1708

Kim, J. W., Lu, Z., Gutenberg, L., & Zhu, Z. L. (2017). Characterizing hydrologic changes of the Great Dismal Swamp using SAR/InSAR. *Remote Sensing of Environment*, *198*, 187–202. https://doi.org/10.1016/j.rse.2017.06.009

Lafleur, P. M., Hember, R. A., Admiral, S. W., & Roulet, N. T. (2005). Annual and seasonal variability in evapotranspiration and water table at a shrub-covered bog in southern Ontario, Canada. *Hydrological Processes*, *19*(18), 3533–3550. https://doi.org/10.1002/hyp.5842

Lafleur, P. M., & Roulet, N. T. (1992). A Comparison of evaporation rates from 2 fens of the Hudson-Bay Lowland. *Aquatic Botany*, *44*(1), 59–69. https://doi.org/10.1016/0304-3770(92)90081-S

Laine, A., Byrne, K. A., Kiely, G., & Tuittila, E. S. (2007). Patterns in vegetation and $CO_2$ dynamics along a water level gradient in a lowland blanket bog. *Ecosystems*, *10*(6), 890–905. https://doi.org/10.1007/s10021-007-9067-2

Lapen, D. R., Price, J. S., & Gilbert, R. (2000). Soil water storage dynamics in peatlands with shallow water tables. *Canadian Journal of Soil Science*, *80*(1), 43–52. https://doi.org/10.4141/S99-007

Lees, K. J., Quaife, T., Artz, R. R. E., Khomik, M., & Clark, J. M. (2018). Potential for using remote sensing to estimate carbon fluxes across northern peatlands—A review. *The Science of the Total Environment*, *2018*(615), 857–874. https://doi.org/10.1016/j.scitotenv.2017.09.103

Lindsay, R. (2018). Peatland classification. In C. Finlayson, et al. (Eds.), *The Wetland Book* (pp. 1515–1528). Dordrecht: Springer. https://doi.org/10.1007/978-90-481-9659-3_341

Liu, L., Zhang, T., & Wahr, J. (2010). InSAR measurements of surface deformation over permafrost on the North Slope of Alaska. *Journal of Geophysical Research*, *115*, F03023. https://doi.org/10.1029/2009JF001547

Mather, P., & Koch, M. (2011). *Computer processing of remotely-sensed images: An Introduction*. New York: John Wiley.

Mathur, A., & Foody, G. M. (2008). Multiclass and binary SVM classification: Implications for training and classification users. *IEEE Geoscience and Remote Sensing Letters*, *5*, 241–245. https://doi.org/10.1109/LGRS.2008.915597

Mezbahuddin, M., Grant, R. F., & Flanagan, L. B. (2016). Modeling hydrological controls on variations in peat water content, water table depth, and surface energy exchange of a boreal western Canadian fen peatland. *Journal of Geophysical Research: Biogeosciences*, *121*, 2216–2242. https://doi.org/10.1002/2016jg003501

Mezbahuddin, M., Grant, R. F., & Flanagan, L. B. (2017). Coupled eco-hydrology and biogeochemistry algorithms enable the simulation of water table depth effects on boreal peatland net $CO_2$ exchange. *Biogeosciences*, *14*(23), 5507–5531. https://doi.org/10.5194/bg-14-5507-2017

Mohammadimanesh, F., Salehi, B., Mahdianpari, M., Brisco, B., & Motagh, M. (2018). Wetland water level monitoring using interferometric synthetic aperture radar (InSAR): A Review. *Canadian Journal of Remote Sensing*, *44*(4), 247–262. https://doi.org/10.1080/07038992.2018.1477680

Moore, T. R., Roulet, N. T., & Waddington, J. M. (1998). Uncertainty in predicting the effect of climatic change on the carbon cycling of Canadian peatlands. *Climatic Change*, *40*(2), 229–245. https://doi.org/10.1023/A:1005408719297

Poore, M. E. D. (1955). The use of phytosociological methods in ecological investigations.1. The Braun-Blanquet system. *Journal of Ecology*, *43*(1), 226–244. https://doi.org/10.2307/2257132

Reeve, A. S., Glaser, P. H., & Rosenberry, D. O. (2013). Seasonal changes in peatland surface elevation recorded at GPS stations in the Red Lake Peatlands, northern Minnesota, USA. *Journal of Geophysical Research: Biogeosciences*, *118*, 1616–1626. https://doi.org/10.1002/2013jg002404

Robinson, E. L., Blyth, E. M., Clark, D. B., Finch, J., & Rudd, A. C. (2017). Trends in atmospheric evaporative demand in Great Britain using high-resolution meteorological data. *Hydrology and Earth System Sciences*, *21*(2), 1189–1224. https://doi.org/10.5194/hess-21-1189-2017

Robroek, B. J. M., Limpens, J., Breeuwer, A., Crushell, P. H., & Schouten, M. G. C. (2007). Interspecific competition between *Sphagnum* mosses at different water tables. *Functional Ecology*, *21*(4), 805–812. https://doi.org/10.1111/j.1365-2435.2007.01269.x

Schwarzel, K., Simunek, J., van Genuchten, M. T., & Wessolek, G. (2006). Measurement and modeling of soil-water dynamics and evapotranspiration of drained peatland soils. *Journal of Plant Nutrition and Soil Science*, *169*(6), 762–774. https://doi.org/10.1002/jpln.200621992

Sowter, A., Amat, M. B., Cigna, F., Marsh, S., Athab, A., & Alshammari, L. (2016). Mexico City land subsidence in 2014-2015 with Sentinel-1 IW TOPS: Results using the Intermittent SBAS (ISBAS) technique. *International Journal of Applied Earth Observation*, *52*, 230–242. https://doi.org/10.1016/j.jag.2016.06.015

Sowter, A., Bateson, L., Strange, P., Ambrose, K., & Syafiudin, M. F. (2013). DInSAR estimation of land motion using intermittent coherence with application to the South Derbyshire and Leicestershire coalfields. *Remote Sensing Letters*, *4*(10), 979–987. https://doi.org/10.1080/2150704x.2013.823673

Waddington, J. M., & McNeill, P. (2002). Peat oxidation in an abandoned cutover peatland. *Canadian Journal of Soil Science*, *82*(3), 279–286. https://doi.org/10.4141/S01-043

Wdowinski, S., & Hong, S.-H. (2015). Wetland InSAR: A Review of the Technique and Applications. In R. W. Tiner, M. W. Lang, & V. V. Klemas (Eds.), *Remote sensing of wetlands: Applications and advances* (pp. 137–154). Boca Raton, USA: CRC Press.

Wosten, J. H. M., Ismail, A. B., & vanWijk, A. L. M. (1997). Peat subsidence and its practical implications: A case study in Malaysia. *Geoderma*, *78*(1-2), 25–36. https://doi.org/10.1016/S0016-7061(97)00013-X

Zhou, Z., Li, Z., Waldron, S., & Tanaka, A. (2016). Monitoring peat subsidence and carbon emission in Indonesia peatlands using InSAR time series, paper presented at 2016 IEEE International Geoscience and Remote Sensing Symposium (IGARSS). https://doi.org/10.1109/IGARSS.2016.7730774